

Dear editor:

Here we submit our revised manuscript for consideration to be published on **Atmospheric Chemistry and Physics**.

The further information about our manuscript is as follows:

Topic: Real-Time Aerosol Optical Properties, Morphology and Mixing States under Clear, Haze and Fog Episodes in the summer of Urban Beijing

Type of Manuscript: article

Authors: Rui Li¹, Yunjie Hu¹, Ling Li¹, Hongbo Fu^{1,2,*}, Jianmin Chen^{1,*}

Corresponding author:

Hongbo Fu; Address: Department of Environmental Science and Engineering, Fudan University, Shanghai 200433, China; Tel.: (+86)21-5566-5189; Fax: (+86)21-6564-2080; Email: fuhb@fudan.edu.cn.

Jianmin Chen; Address: Department of Environmental Science and Engineering, Fudan University, Shanghai 200433, China; Tel.: (+86)21-5566-5189; Fax: (+86)21-6564-2080; Email: jmchen@fudan.edu.cn

Firstly, we acknowledge the comments of anonymous reviewers, and are also grateful to the efficient serving of the editor. We have already revised MS based on the reviewers' comments. We also inspected MS roundly and corrected some errors in English presentation. We are sure that the revised MS adhere to **Atmospheric Chemistry and Physics** format. The marked MS was also uploaded to be easily reviewed.

#Reviewer 1

Comment:

1. The English thorough the manuscript are suggested to be improved by an English native speaker.

Response:

The English thorough the manuscript have been improved by an English native speaker.

Comment:

2. The abstract immediately begins with specific results, without providing an overview of the study or its objectives.

Response:

Line 12-14: Indeed, an overview of the study or its objectives should be provided in the abstract. Thus, “Aerosol particles play significant roles on the climate-forcing agent via its optical absorption properties. However, the relationship between characteristics of aerosol particles and optical absorption remains poorly understood” has been added in the abstract.

Comment:

3. Line 28: Please give a definition of soot fog period.

Response:

Line 36: “Soot fog period” means the fog episode filled with large amount of soot.

Comment:

4. Line 284: the abbreviate of correlation coefficient is “r” not “R”. The valid number thorough the manuscript should be consistent.

Response:

Line 290: “R” has been changed into “r”.

Comment:

5. Is “organic matter” a right expression? Tar ball and soot are also organic matter. The statement that organic matter could be traced to the direct emission such as biomass burning or the second reaction between the VOCs with ozone is speculative. More discussion should be conducted to demonstrate this statement.

Response:

“organic matter” is a right expression, which has much difference from soot and tar ball. Li et al. (2009) and Fu et al. (2012) also used “organic matter” expression in their paper. Organic matter generally exhibits amorphous structure with abundant carbon and minor oxygen, whereas soot are chain-like aggregates of carbon-bearing spheres. Tar ball displays spherical appearance with substantial carbon, while they generally do not possess other elements. Organic matter could be released via biomass burning, vehicle exhausts, and other human activities by directly process. Besides, they can also be generated through photochemical reaction between VOCs and some photochemical oxidants such as O₃ and NO_x.

Comment:

6. How does the cubic shape of K-rich particles suggested they have not undergone long transportation? More clarification needed.

Line 357: The cubic shape of K-rich particles suggested they have not undergone long transportation or severe photochemical reaction because cubic K-rich particles were mainly produced from the molten nature of the material at high temperatures. The K-rich particles undergoing the long-range transport are generally encapsulated by visible coatings.

Comment:

7. TEM analysis can only observe limited amount of particles. Could you assure the quality of the data?

Response:

Indeed, coarser particles were near the centers of the grid and finer particles on the periphery. However, three to four areas were chosen from the center and periphery of the sampling spot on each grid in order to ensure that the analyzed particles were representative. Therefore, we can assure the quality of the data.

Comment:

8. More literature published after 2016 about the optical properties should be cited.

Response:

Much literature published after 2016 about optical properties has been cited, which was marked in red characters in the revised version.

#Reviewer 2

Comments:

1. The English thorough the whole manuscript should be improved by a native English speaker.

Response:

The English thorough the manuscript have been improved by an English native speaker.

Comments:

2. More recent reports about the influence of agricultural activities including biomass burning on the regional air quality are encouraged to be cited.

Response:

Many new published paper have been added into the manuscript.

Comments:

3. Abstract: Line 12-16, the sentences are suggested to be replaced by “Aerosol optical properties and morphologies were measured by TEM, CRDS, a nephelometer and an aethalometer in a urban site of Beijing from 24 May to 22 June”. The clear, haze and fog episodes just occurred during the sampling period, it didn’t need to mention them in the abstract. The phrase of “sampled from...” is not correct in English grammar. The instruments were used for measuring the aerosol properties, but not for investigating the corresponding changes of the aerosol properties. Line 16- 17, the sentence is meaningless, because the individual episode was mentioned in the following sentences. Line 17-18, the phrase of “which are mostly externally mixed” is not clear, and hence suggested to be changed as “and the particles were mostly mostly externally mixed”. Line 20-21, the comma before which should be deleted, because the phrase is used for modifying the EP-4. Line 21-22, “industry-induced haze (EP-1) and biomass burning-induce haze (EP-5)” is suggested to be changed as “the industryinduced pollution episode (EP-1) and biomass burning-induce pollution episode (EP-5)”. Line 22-24, The two sentences seemed to be independent, lack of logic, and thus, the two sentences are suggested to be replaced by “Compared with the EP-2 and EP-4, the AOD values and the size distribution of particles during EP-1 and EP-5 were much greater because of relatively high particle concentrations ”. Line25-26, the sentence was suggested to be replaced by “In contrast to the EP-1, a large fraction of soot which sticks to KCl, sulphate or nitrate particles was detected during the EP-5”, implying the evident influence of severe crop residue combustion. Line 26-28, the sentence was suggested to be replaced by “Additionally, evident enhancement of light absorption was observed during the EP-5, which was mainly ascribed to both BC acceleration and other

absorbing substances”. Line 28-31, the sentences are better replaced by “However, soot was found mostly internally mixed with sulphate and nitrate during a soot fog episode (EP-3), resulting in evident enhancement of light absorption”.

Response:

Line 14 - 16: The sentences have been changed into “Aerosol optical properties and morphologies were measured by TEM, CRDS, a nephelometer and an aethalometer in a urban site of Beijing from 24 May to 22 June”.

Line 16-20: Indeed, the sentence is meaningless and has been deleted.

Line 23: “which” was replaced by “and the particles”. The comma has been deleted

Line 27: the sentences has been changed into “industry-induced haze (EP-1) and biomass burning-induced haze (EP-5) were both affected by the south air mass”.

Line 28: The two sentences have been replaced by “Compared with the EP-2 and EP-4, the AOD values and the size distribution of particles during EP-1 and EP-5 were much greater because of relatively high particle concentrations.”

Line 32: The sentence was replaced by “In contrast to the EP-1, a large fraction of soot which sticks to KCl, sulphate or nitrate particles was detected during the EP-5”.

Line 33: The sentence was replaced by “Additionally, evident enhancement of light absorption was observed during the EP-5, which was mainly ascribed to both BC acceleration and other absorbing substances”.

Line 35: The sentence has been changed into “However, soot was found mostly internally mixed with sulphate and nitrate during a soot fog episode (EP-3), resulting in evident enhancement of light absorption”.

Comments:

4. Line 44-47, any kind of particles in the atmosphere have scattering effect, why did you only stress on inorganic salts and light-color organic carbon? The sentences is better replaced by “inorganic salts and light-color organic carbon have a “cooling effect” on climate due to decreasing permeation of solar irradiation onto the Earth’s surface through solely scattering sun light”. There are still some sentences in the section being needed to be improved.

Response:

Line 53-54: Indeed, the sentence has been changed into “inorganic salts and light-color organic carbon have a cooling effect”.

Comments:

5. Line 266-267, the sentence of “the north wind was relatively clean and the time was insufficient for a heavy accumulation” is not proper and clear. Wind can be only described by speed and direction, and hence the sentence is better replaced by “the air parcel from the North was relatively clean”. What’s “the time” in the latter half sentence”? Line 282, the title of “Optical parameter variation” is better replaced by “The variation of aerosol optical characters”. Line 324, the title of “TEM analysis” is suggested to be “Morphology and chemical composition of aerosols”. Line 319: “Especially when air masses moved from south direction to the sampling site aerosols were influenced by heavy soot-sulfate-OC-mixed pollution”. How did you draw the conclusion? Line 388: Are you sure haze and fog episodes had a high possibility of collision just due to the heavy particle loading? You should add relevant reference to confirm your deduction. Line 390, the title of “Optical properties related to morphological of aerosols” is better replaced by “the relationship between the aerosol optical properties and morphologies”.

Response:

Line 273: The sentence was changed into “the air parcel from the North was relatively clean”.

Line 288: The sentence was changed into “The variation of aerosol optical characters”

Title 3.3: The title was replaced by “Morphology and chemical composition of aerosols”

Line 328: The conclusion was drawn because some previous studies have confirmed that soot, organic matter, and sulfates were generated from the industrial activities, domestic cooking, and biomass burning. Many industrial activities and biomass burning have been observed in South China.

Line 397: Haze and fog episodes generally had a high possibility of collision, which was caused by heavy particle loading. In addition, prolonged remaining of heavy particles was also a factor leading to the collision. Many relevant references have been added in the manuscript.

Line 407: The title was replaced by “Optical properties related to morphological types of aerosols”.

#Reviewer 3

Comment 1:

Line 259-260: The time range mentioned here is from 28 th May to 29 th May, but in Figure 1, it is from 24th May to 29th May. Please check and keep in consistency.

Response:

Line 266: The time range mentioned here is from 24 th May to 29 th May after the careful check.

Thus, the “28 th” has been changed into “24 th”. Thank you for reviewer’s chariness.

Comment 2:

Line 284: How do you obtain the value $R=0.603$.

Response:

Line 299: The R value was obtained using Pearson correlation analysis. The R value is the correlation coefficient between AOD and PM_{10} with a 95% confidence interval.

Comment 3:

Line 385-389: There might be a misunderstanding of the definition of the internal and external mixing stages. The adjacent particles belong to the category of “inhomogeneous” internal mixing. Please refer to the relative papers for the definition.

Response:

Indeed, adjacent particles belong to the category of inhomogeneous internal mixing after my critical review of references. Therefore, the “internal” and “adjacent” were replaced by “internal” and “internal (adjacent)” in Fig. 5, respectively.

Comment 4:

Line 390: the title of this section may be changed into “Optical properties related to morphological types of aerosols”.

Response:

Line 401: The title has been changed into “Optical properties related to morphological types of aerosols”.

Comment 5:

Line 700: The meaning of “No.” in Table 1 is not clear.

Response:

Table 1: The title has been replaced by “Sampling time and instantaneous meteorological state”.

Comment 6:

Line 710-713: It seems this is not Figure 3, instead, it may be Figure 6. Similarly, Figure 5 in Line 717-720 might be Figure 3, and Figure 6 in Line 721-722 might be Figure 5. Please check this section.

Response:

Fig 3-6: The figure caption is confused, and right figure caption was added in the manuscript.

Comment 7:

Line 726 Figure 1: The keys for this diagram are not very clear. The upper one: in addition to rain, fog, and haze days, the clear days should be expressed in white color key. The middle one: what are the meanings of the grey color and orange color?

Response:

Fig. 1: In the upper diagram, the color column has been added. In the middle one, brown, green, and orange color meant the haze, clear, and fog conditions, respectively, which were added in the figure caption.

Comment 8:

Line 738 Figure 2: Keys for this diagram should be added. What are represented by those different colors of lines?

Response:

Fig. 2: Green, purple, red, and blue line denotes the air parcel with the height of 500, 1000, 2000, and 3000 m, which was added in the figure caption.

Comment 9:

Line 748 Figure 3: Keys in figure 3c are erroneously used. The figure is not consistent with the description in text of Line 187-188.

Response:

Fig. 3: I think the Fig. 3 is consistent with the description in text of Line 187-188, no contradictory description was observed.

Comment 10:

Line 761 Figure 5: The values in the vertical axis should be 20, 40, 60, 80, and 100 percentages.

Besides, are the percentages in this diagram based on statistics of the area or number? What about the values of the rainy days?

Response:

Fig. 5: The percentage in this diagram was obtained based on statistics of number. The main aim of our study is to compare the optical properties and morphologies of particles among haze, fog, and clear, and then decipher the relationship between optical properties and morphologies. However, the optical property and morphology in the rainy days were not set as our main objectives. Thus, the percentage of particles in the rainy days were not included in Fig. 5.

Comment 11:

Figure 6: The types in the classification shown in this figure are not consistent with those in Figure 4. The mineral particle type is missing in Figure 6, and still in this figure, the values of the rainy days are missing as well.

Response:

Fig. 6: the Ca-S particles and rod belong the same class. The Ca-S particles were changed into mineral and rod was replaced by Ca-S particles. The particles in the rainy days were not included in our study.

Comment 12:

The keys in Figure 1, 3, and 7 should include those of the clear days (for those white areas). Also, the data for the clear days should be added.

Response:

Fig. 1, 3, and 7: the white color has been added in the revised version.

1 **Real-Time Aerosol Optical Properties, Morphology and Mixing**
2 **States under Clear, Haze and Fog Episodes in the summer of Urban**
3 **Beijing**

4 Rui Li¹, Yunjie Hu¹, Ling Li¹, Hongbo Fu^{1,2,*}, Jianmin Chen^{1,*}

5 ¹ *Shanghai Key Laboratory of Atmospheric Particle Pollution and Prevention, Department of*
6 *Environmental Science & Engineering, Fudan University, Shanghai 200433, China Chinese*
7 *Academy of Sciences, Institute of Atmosphere Physics, Beijing 100029.*

8 ² *Collaborative Innovation Center of Atmospheric Environment and Equipment Technology*
9 *(CICAET), Nanjing University of Information Science and Technology, Nanjing 210044,*
10 *China*

11 **Abstract**

12 Aerosol particles play significant roles on the climate-forcing agent via its optical absorption
13 properties. However, the relationship between characteristics of aerosol particles and optical
14 absorption remains poorly understood. Aerosol optical properties and morphologies were
15 measured by TEM, CRDS, a nephelometer and an aethalometer in a urban site of Beijing from
16 24 May to 22 June. ~~Characteristics of aerosol optical properties, morphologies and their~~
17 ~~relationship were studied in urban Beijing during the clear, haze and fog episodes, sampled~~
18 ~~from 24th May to 22nd Jun, 2012. Transmission Electron Microscope (TEM), a Cavity Ring~~
19 ~~Down Spectrometer (CRDS), a nephelometer and an aethalometer were employed to~~
20 ~~investigate the corresponding changes of the aerosol properties.~~ Five episodes were categorised
21 according to the meteorological conditions and composition. The results showed that the clear

22 episode (EP-2 and EP-4) featured as the low Aerosol Optical Depth (AOD = 0.72) and less
23 pollutants compared with haze (1.14) and fog (2.92) episodes and the particles are mostly
24 externally mixed. The high Ångström exponent (> 2.0) suggests that coarse particles were
25 scarcely observed in EP-2 due to the washout of a previous heavy rain, whereas they were
26 widespread in EP-4 (Ångström exponent = 0.04), which had some mineral particles introduced
27 from the north. In contrast, industry-induced haze (EP-1) and biomass burning-induced haze
28 (EP-5) were both affected by the south air mass. Compared with the EP-2 and EP-4, the AOD
29 values and the size distribution of particles during EP-1 and EP-5 were much greater because
30 of relatively high particle concentrations. All of the particles were classified into nine categories
31 including S-rich, N-rich, mineral, K-rich, soot, tar ball, organic, metal and fly ash on the basis
32 of TEM analysis. In contrast to the EP-1, a large fraction of soot, which sticks to KCl, sulphate
33 or nitrate particles were detected during the EP-5. Additionally, evident enhancement of light
34 absorption was observed during the EP-5, which was mainly ascribed to both BC acceleration
35 and other absorbing substances. However, soot was found mostly internally mixed with
36 sulphate and nitrate during a soot fog episode (EP-3), resulting in evident enhancement of light
37 absorption. The larger size distribution was likely to be caused by both hygroscopic growth and
38 collision between particles during the aging. About 28% of particles were internally mixed in
39 the foggy days, which favored the light absorption. The comparison of all the episodes provides
40 a deeper insight of how mixing states influence the aerosol extinction properties and also a clue
41 to the air pollution control in the crop burning seasons.

42 **Keywords:**

43 Aerosol optical depth, Ångström exponents, Single scattering albedo, Transmission Electron
44 Microscope, Biomass burning, Soot

45 **1. Introduction**

46 Aerosol particles are ubiquitous in the troposphere and exert an important influence on global
47 climate and the environment (Ramana et al., 2010). They affect climate through direct
48 scattering, transmission, and absorption of radiation, or indirectly by acting as nuclei for cloud
49 formation (Buseck and Posfai, 1999). In addition, light extinction by aerosol particles can
50 impair visibility, both during extreme events such as dust storms, and more widely in the
51 vicinity of urban regions, frequently leading to regional haze and fog events (Wang et al., 2009a;
52 Chameides et al., 1999; Sun et al., 2006; Saleh et al., 2016). **Inorganic salts and light-color
53 organic carbon have a “cooling effect” on the climate due to a decrease in the solar radiation
54 that reaches the Earth’s surface** (Buseck and POsfai, 1999). Soot aerosols, mineral dust, and
55 brown carbon are important absorbing aerosols that can lead to global and regional warming
56 effects (Buseck and Posfai, 1999; Bahadur et al., 2012; Wang et al., 2014). The impact of
57 aerosols on the Earth’s climate is a major uncertainty in climate change models as was
58 emphasized in the latest Intergovernmental Panel on Climate Change (IPCC) report (Solomon,
59 2007). It follows that understanding aerosol optical behaviour and associated spatial and
60 temporal variability is a necessary prerequisite to understanding its role in climate and the
61 environment (Langridge et al., 2012; Che et al., 2014). Soot is a major contributor to Earth’s
62 radiative balance (Ramana et al., 2010). Recent investigations involving direct atmospheric
63 measurements of soot aerosols suggest that they may have a global warming potential second

64 only to CO₂, and the warming effect by soot nearly balances the net cooling effect of other
65 anthropogenic aerosols (Jacobson, 2001). Not surprisingly, the importance of soot to climate
66 change has been a major focus of many modelling, laboratory, and field studies (Zhang et al.,
67 2008;Adler et al., 2010;Moffet and Prather, 2009;Adachi and Buseck, 2008;Ram et al., 2012).
68 The main uncertainty stems from the fact that the actual amount soot warms our atmosphere
69 strongly depends on the manner and degree in which it is mixed with other species, a property
70 referred to as mixing state (Jacobson, 2001;Moffet and Prather, 2009). The mixing state was
71 found to affect the soot global direct forcing by a factor of 2.9. It has been shown that absorption
72 by soot increases when soot particles are internally mixed and/or coated with other less
73 absorbing materials (Moffet and Prather, 2009). This enhanced absorption in such structure is
74 because of the lensing effect of coated materials (Jacobson, 2001). Field measurements indicate
75 that during transport from the sources, fresh soot becomes internally mixed with sulphate and
76 organics, leading to enhancement in light absorption, which confirms the modelling calculation
77 (Kleinman et al., 2007;Doran et al., 2007;Carabali et al., 2012). Kleinman et al. observed a
78 doubling in the ratio of aerosol light absorption in aged air masses compared to fresh emissions
79 over the eastern U.S. (Kleinman et al., 2007). Similar increases in absorption by soot-bearing
80 aerosol have been reported from ground site measurements performed at a series of locations
81 downwind of Mexico City (Doran et al., 2007). Compiling both the surface and aircraft
82 measurements, Ramana et al. recommended that the solar-absorption efficiency of the Beijing
83 and Shanghai plumes was positively correlated with the ratio of soot to sulphate (Ramana et al.,
84 2010). Lei et al. further confirmed that the enhanced absorption of mixed aerosols depended

85 upon hygroscopicity and the thickness of the coating (Lei et al., 2014). Based on the combined
86 proof from the modelling and field studies, most of researchers proposed that internal mixing
87 models of soot present more realistic absorption estimates as compared to external mixing
88 models in which soot particles coexist with other particles in a physically separated manner
89 (Jacobson, 2001; Ramana et al., 2010; Lei et al., 2014).

90 Biomass burning is by far the largest source of primary, fine carbonaceous aerosols in the
91 atmosphere (Habib et al., 2008). It is estimated to contribute 20% of soot aerosols from biomass
92 burning. Besides strongly absorbing soot particles, high amounts of brown organic carbon, such
93 as “tar ball” or HULIS, can be emitted from biomass burning (Roden et al., 2006; Hand et al.,
94 2005; Hoffer et al., 2006). Brown carbon has a significant absorbing component at short
95 wavelengths that may be comparable to the soot absorption (Alexander et al., 2008; Bahadur et
96 al., 2012). Consequently, organic carbon from biomass burning may also contribute to the
97 warming potential of aerosols (Alexander et al., 2008). These large quantities of climate-related
98 aerosols can persist in the atmosphere for several weeks and be transported over long distances.
99 As a result, biomass burning aerosols have a significant impact on climate, which was
100 considered to provide a major uncertainty in accurately predicting the effects of light-absorbing
101 aerosols on the climate (Bahadur et al., 2012). Many field measurements in East Asia, South
102 Asia and Africa have shown extensive biomass burning in these regions causes important
103 perturbations to Earth’s atmosphere (Gustafsson et al., 2009; Alexander et al., 2008; Hand et
104 al., 2005). Once biomass burning particles are mixed with other atmospheric components
105 during aging and transport, such as sulfate and dust, solar absorption is further amplified due

106 to the formation of internally mixed particles (Ramanathan et al., 2005). Such mixtures of
107 absorbing and scattering aerosols at the regional scale are referred to as ABCs, for atmospheric
108 brown clouds (Ramanathan et al., 2007). ABCs radiative forcing can cool the surface, stabilize
109 the atmosphere, and reduce evaporation and monsoonal rainfall. The large influence of ABCs
110 on the climate and hydrological cycle changes has recently been demonstrated through model
111 simulations (Ramanathan et al., 2007; Ramanathan et al., 2005).

112 In the farmlands of eastern China such as that near Beijing, most wheat straw is burned in
113 the field within one week after harvesting in preparation for rice cultivation during May and
114 June. Emissions from the biomass burning are often transported and mixed with urban pollution,
115 leading to degradation of air quality, visibility impairment, and regional haze events (Li et al.,
116 2010). Stagnation occurs during episodes of urban haze, when there is insufficient wind
117 velocity to carry pollutants away from the city (Katrinak et al., 1993; Sun et al., 2006). During
118 these periods of pollutant retention, haze particles aggregate continue to collide and combine,
119 resulting in larger average sizes and altered morphology (Li et al., 2010). Enhanced absorption
120 is mainly brought about in the presence of high levels of non-absorbing hygroscopic aerosols
121 such as sulphates, nitrates, and water-soluble organic carbon, as their hygroscopic nature favors
122 internal mixing/core-shell formation (Bahadur et al., 2012). On the other hand, under the
123 condition of high atmospheric relative humidity (RH), the initially hydrophobic soot particles
124 can become associated with hygroscopic materials, leading to increased scattering due to
125 particle growth. At an extreme case, the coating material can cause the absorbing fractal soot
126 to collapse, potentially changing optical behaviour, to further complicate this picture (Zhang et

127 al., 2008; Langridge et al., 2012; Lei et al., 2014; Tan et al., 2016). Such changes cause both
128 positive and negative effects on the interplay between the direct and indirect aerosol effects,
129 making overall prediction of the radiative forcing difficult. Up to date, large uncertainties exist
130 in estimates of the radiative forcing of haze particles because of the lack of detailed in situ
131 measurements of the mixing state and the associated optical properties as a function of particle
132 size and composition (Moffet and Prather, 2009). These uncertainties limit our ability to
133 quantify the relative impacts of soot on climate, thus limiting our ability to make effective
134 policy decisions.

135 In an attempt to address this knowledge gap, and in the absence of the opportunity for
136 widespread field studies in eastern China, the experiments in this study were designed to
137 simultaneously measure mixing states and optical properties of haze particles. The present
138 analysis focused on the Beijing plume, which in addition to strong urban emissions is
139 influenced by local agricultural emissions (Li et al., 2010). Light extinction and scattering
140 coefficient was measure with a cavity ring-down spectrometer (CRDs) and a nephelometer,
141 respectively. Absorption was calculated from the difference between extinction and scattering.
142 Individual aerosol particles were identified with transmission electron microscopy (TEM).
143 Back trajectory analyses suggest flow patterns consistent with long-range transport of
144 agricultural smoke to the study site during periods when the sampling site was engulfed by the
145 serious haze and fog.

146 **2. Experimental Sections.**

147 **2.1 site description**

148 All of ambient investigation of aerosol optical properties and TEM samplings were
149 conducted at the Institution of Atmospheric Physics (39°58'N, 116°22'N), Beijing, China, from
150 24th May to 22nd Jun, 2012. Samplers were mounted on the roof of a two-story building about
151 8 m above ground level. The surroundings are in the convergence of residential and commercial
152 zones with some steel plants locating around in a distance of 6 to 25 km and a waste incineration
153 facility (Gaodun) 8 km in the northeast, which has an operational capacity of 1600 t d⁻¹. In
154 addition, the sampling site is suited in the middle of the North Third Ring Road and North
155 Fourth Ring Road, approximately 360 m south and 380 m north, respectively. The sampling
156 site is impacted by the mixture of residential, industrial, waste combustion and vehicle
157 emissions, but not dominated by any one source.

158 **2.2 Cavity ring-down spectrometer and nephelometer**

159 A self-designed cavity ring-down spectrometer (CRDS) was performed to measure the
160 extinction coefficient of aerosols at 1 min intervals with an accuracy of 0.1 Mm⁻¹. Aerosols
161 were dried by diffusion drying tubes before they reached CRDS and Nephelometer to exclude
162 the influence of relative humidity (RH) on the aerosol optical properties. RH was kept below
163 40% to minimize the effects of changing RH on measurements. The cavity was formed by two
164 high-reflectivity dielectric mirrors (Los Gatos Research, Inc., Mountain View, CA, USA) and
165 a stainless steel cell equipped with two inlets at both ends and one outlet in the middle. The
166 entire distance of two mirrors is 76.4 cm, while the filling length is 58.0 cm. Dry nitrogen
167 was released near the mirrors at a flow of 0.03 L min⁻¹ to prevent the contamination of mirrors
168 and aerosol flow was set 1.0 L min⁻¹. The 532 nm light pulse (energy 100 μJ, duration 11 ns)

169 was generated by a Q-switched pulsed laser (CrystaLaser QG-532-500). Leaking light through
170 the mirrors was monitored by a Hamamatsu R928 photomultiplier. Details about the system
171 were reported by Li et al (2011). To calculate the decay time, 1000 ring-down traces were
172 averaged at 1000 Hz repetition rate. The extinction coefficient (α_{ext}) has an uncertainty below
173 3% under the controlled conditions. It was calculated according to the following equation:

$$\alpha_{ext} = \frac{L}{lc} \left(\frac{1}{\tau} - \frac{1}{\tau_0} \right) \quad (1)$$

174

175 Where L is the length of the cavity, l is effective length occupied by particles, c is the speed of light, τ_0
 176 is ring-time time of the cavity filled with particle-free air and τ is the calculated decay time (Li et al.,
 177 2011).

178 An integrating nephelometer (TSI, Model 3563) was operated to obtain aerosol scattering coefficient at
 179 three different wavelengths (450, 550, and 700 nm) and the flow rate was set at 5 L min⁻¹. During the field
 180 campaign, zero check was done automatically by pumping in particle-free air for 5 min once every 2 h, and
 181 a span check was conducted manually using CO₂ as the high span gas and filtered air as the low span gas
 182 every week. RH was kept below 40% to minimize the effects of changing RH on measurements (Peppler
 183 et al., 2000; Clarke et al., 2007). The raw data were corrected for truncation errors and a non-Lambertian
 184 light source using Ångström exponents (\hat{a}) according to Anderson and Ogren (1998) (Anderson and Ogren,
 185 1998). Generally, the total uncertainty of the scattering coefficient (α_{scat}) was generally below 10%. In
 186 accordance with the extinction coefficient at 532 nm, the scattering coefficients was
 187 converted to 532 nm ($\alpha_{scat,532}$) on the basis of the following equation:

$$\alpha_{scat,532} = \alpha_{scat,\lambda} \left(\frac{532}{\lambda} \right)^{-\hat{a}} \quad (2)$$

188

189 Where $\alpha_{scat,\lambda}$ is the scattering coefficient at the wavelength of λ . Accordingly, \hat{a} could be computed
 190 calculated as the equation (3),

$$\hat{a} = - \frac{\lg(\alpha_{scat,\lambda_1} / \alpha_{scat,\lambda_2})}{\lg(\lambda_1 / \lambda_2)} \quad (3)$$

191

192 and the single scattering albedo (ω_0) at the given wavelength could be calculated from equation (4),

193

$$\omega_0 = \frac{\alpha_{scat}}{\alpha_{ext}} \quad (4)$$

194 As the sum of absorption (α_{abs}) and scattering (α_{scat}) coefficients equals the extinction coefficient (α_{ext}),
195 α_{abs} could be derived from the equation (5),

196
$$\alpha_{abs} = \alpha_{ext} - \alpha_{scat} \quad (5)$$

197 It is known that RH also has a profound impact on visibility (Chow et al., 2002), however, in this study the
198 aerosols passed through a diffusion drying tube before the measurement of optical properties, thus aerosol
199 optical property measurements and TEM observations were both performed in dry condition.

200 **2.3 Aethalometer**

201 An Aethalometer (model AE-31, Magee Scientific Company) was employed to simultaneously quantify
202 BC concentration by calculating the optical attenuation (absorbance) of light from light emitting diode
203 lamps emitting at seven different wavelengths (370, 470, 520, 590, 660, 880 and 950 nm) every 5 minutes,
204 with a typical half-width of 0.02 μm (Hansen, 2003). The flow rate was set to be 5 L min^{-1} and a clean filter
205 canister in the inlet was used weekly to conduct the zero calibration. A $\text{PM}_{2.5}$ cyclone (BGI SCC 1.828)
206 was employed in the sampling line with a flow rate of 5 L min^{-1} . A typical noise level is less than 0.1 μg
207 cm^{-3} on a 5-min basis. Two photo-detectors monitor the light intensity as a function of time. One measured
208 the light intensity of the light crossing reference quartz filter, while the other measured that of the same
209 light crossing a sample spot under the identical conditions. The wavelength at 880 nm was used to derive
210 the aerosol absorption coefficient (σ_{abs}). Then BC concentration could be converted under the assumption
211 that the BC mass concentration [BC] on the filter was linearly correlated to the aerosol absorption
212 coefficient, as the following equation (6),

213
$$\sigma_{abs} = \alpha[BC] \quad (6)$$

214 Where [BC] is the BC mass concentration, and α is a conversion factor. A factor of 8.28 $\text{m}^2 \text{g}^{-1}$ was
215 employed to convert the aerosol absorption coefficient to BC concentration, according to the results of
216 inter-comparison experiment conducted in south China (Wu et al., 2009; Yan et al., 2008).

217 The uncertainty of measurement might originate from the multiple scattering in the filter fibres in the
218 unloaded filter and in those particles embedded in the filters (Clarke et al., 2007; Jeong et al., 2004). The

219 attenuation values were within the limit of an acceptable uncertainty, that is, no greater than 150 in the
220 range of 75-125 at various wavelengths, verifying the reliability of the measurement. Moreover, the BC
221 concentration was compared with the results of multi-angle absorption photometry (MAAP, Model-5012)
222 and a particle soot absorption photometer (PSAP, Radiance Research), which shows great consistence.

223 **2.4 Aerosol optical depth**

224 Aerosol optical depth (AOD) data at the sampling site was based on the MODIS (Moderate Resolution
225 Imaging Spectroradiometer) retrieved data from a CIMEL CE-318 sunphotometer (AERONET/PHOTONS)
226 at Institute of Atmospheric Physics, reflecting the amount of direct sunlight prevented from reaching the
227 ground by aerosol particles by measuring the extinction of the solar beam. The AOD value of the sampling
228 site was downloaded from the AERONET (<http://aeronet.gsfc.nasa.gov>), using the Level 2.0. Quality
229 Assured Data. These data are pre and post field calibrated, automatically cloud cleared and manually
230 inspected. The regional distribution of AOD was obtained from Giovanni (GES-DISC Interactive Online
231 Visualization And Analysis Infrastructure) maps from MODIS satellite data
232 (<http://disc.sci.gsfc.nasa.gov/giovanni>). Two continuous episodes featuring as clear and haze are chosen,
233 23th May to 27th May and 19th June to 27th June, respectively.

234 **2.5 TEM Analysis**

235 Samples were made by collecting air-borne particles onto copper TEM grids coated with carbon film
236 (carbon type-B, 300-mesh copper, Tianld Co., China) using a single-stage cascade impactor with a 0.5 mm
237 diameter jet nozzle at a flow rate of 1.0 L·min⁻¹. According to the visibility, the sampling time varies from
238 1 min to 10 min. 3 or 4 samples were collected each morning at around 8 am and also each time when haze
239 or fog appeared. After collection, samples were stored in a dry plastic box sealed in a plastic bag and kept
240 in a desiccator at 25 °C and 20 ± 3%. Details of the analysed samples, such as sampling time and
241 instantaneous meteorological state are listed in Table 1.

242 Individual aerosol samples were analysed using a high resolution TEM (JEOL 2010, Japan) operated at
243 200 kV. TEM can obtain morphology, size, and mixing state of individual aerosol particles. Energy-
244 dispersive X-ray spectrometer (EDS) can get the chemical compositions of the targeted particles. Cu and C

245 were excluded from the copper TEM grid with carbon film. Details have been described in the previous
246 paper (Fu et al., 2012; Guo et al., 2014a). Particle sizes on the grid decrease from the centre to the periphery
247 due to the limitation of sampler, and three to four round meshes were chosen from the centre to the periphery
248 in a line to ensure the representative of the entire size range. Each mesh analyses three to four views. The
249 average values of each mesh were used for statistics. The analysis was done by labour-intensive manual
250 sortation of the particles. 9 grids, all of 1173 particles have been analysed by TEM.

251 **2.6 Back trajectories and meteorological data**

252 NOAA/ARL Hybrid Single-Particle Lagrangian Integrated Trajectory model (available at
253 <http://www.arl.noaa.gov/ready/hysplit4.html>) was employed to determine back trajectories arriving at
254 Beijing at 100 m, employing the data of global data assimilation system (GDAS). Each trajectory
255 represented the past 72 h of the air mass, with its arrival time at 00:00 UTC every day.

256 Meteorological data was downloaded from Weather Underground (www.wunderground.com), and Daily
257 PM₁₀ values were transformed from daily API (Air Pollutant Index) in the datacentre of ministry of
258 Environmental Protection of the People's Republic of China (<http://datacenter.mep.gov.cn/>).

259 **3. Results and Discussion**

260 **3.1 Episode segregations**

261 Haze was usually defined as a weather phenomenon that lasts a duration of at least 4 h when the visibility
262 is less than 10 km and RH lower than 80% (Sun et al., 2006), while fog was characterized with a higher
263 RH, larger than 90%, according to the Chinese Meteorological Administration. The sampling period was
264 categorized into 5 episodes to observe the optical properties between different weather phenomena (Fig. 1).
265 Although every episode contains a mixture of different pollutions, the main origin can be discerned by
266 studying the weather condition, back trajectories and fire maps. The 1st episode (EP-1) was from 24th
267 May to 29th May, when a haze occurred with the south wind bringing in the industrial pollution from the
268 heavily polluted cities in the south, which conformed to the 3-day back trajectories shown in Fig. 2a,
269 showing the air masses passing through Henan, Shandong, Hebei and Tianjin before arriving at the
270 sampling site. Only scattered fire spots were observed during these days along the air mass pathway,

271 suggesting little biomass burning emission interference. The 2nd episode (EP-2) was in clear weather on
272 30th May. A heavy rain interrupted the previous haze; hence the air were cleaned up by rain washout. It
273 was impacted by the air mass from the north region (Fig. 2b), as the air parcel from the North was relatively
274 clean and the time was insufficient for a heavy accumulation. This episode could be viewed as the
275 background. The 3rd episode (EP-3) from 31st May to 9th Jun was fickle, with a variety of transitions
276 between fog, haze and clear days. This was partly caused by the variable wind directions and air mass
277 transferring (Fig. 2c). When the wind is from east, the back trajectories are across the Bohai Sea, and the
278 air mass carries a high content of water vapour, facilitating the formation of fog, whereas when south wind
279 is dominant, haze is likely to occur (Wang and Chen, 2014;Zhang et al., 2010). The following 4th episode
280 (EP-4) from 10th Jun to 16th Jun is mainly clear days with slight dust. Their back trajectories originate
281 from the north part (Fig. 2d), and mostly travelling from the Siberian region, across eastern Mongolia and
282 Inner Mongolia and finally arriving the sampling site with little pollution. The last episode (EP-5) was from
283 17th Jun to 21st Jun. Severe haze was observed during this duration. Fig. 2e shows that the air parcel
284 pathway across by dense fire spots, indicating a severe impact of the biomass burning. Every year after
285 harvest, crop residue burning is extremely frequent in Anhui, Shandong and Henan provinces as they served
286 as important centres for the rice supply (Li et al., 2010). Therefore, the biomass burning emissions can be
287 the main contributor to the haze formation in this episode.

288 **3.2 The variation of aerosol optical characters**

289 Aerosol optical depth (AOD) is representative of the airborne aerosol loading in the atmospheric column,
290 which was also verified by a significant related coefficient with PM_{10} ($r=0.603$) (Fig. 1). The overall AOD
291 is contributed by both Mie scatter and Rayleigh scatter (Fig. 3a). The former one is produced by the scatter
292 effect of particles while the latter one by gases (Brown et al., 2014). The data shown in Fig. 1 demonstrates
293 that gas plays a negligible role in the AOD value, especially when aerosol loading is high. Apparently, the
294 AOD value varied with the weather transition. During the clean days, the mean AOD was 0.723, while it
295 became higher when the haze and fog were formed, with a mean value of 2.92 and 1.14, respectively.

296 During the measurement period, AOD reached its highest value of 5.0 in the hazy EP-5, which was much
297 higher by 5 times than the average AOD of 0.95 in Beijing measured from Mar 2012 to Feb 2013 (Guo et
298 al., 2014b). Such high AOD could be attributed to the pollutant accumulation, especially biomass burning
299 emission from the crop combustion.

300 Ångström exponent (\AA) is a good indicator of aerosol size distribution, which decreases with the increase
301 of particle size (Eck et al., 1999). The value is computed from pairs of AOD measurements at 700 nm with
302 450 nm, 700 nm with 550 nm and 550 nm with 450 nm, respectively. A high accordance is observed
303 between each pair (Fig. 3b). The \AA increases sharply to its highest value above 2.0 at EP-2, 45 times of the
304 minimum value 0.044 observed in EP-5. This could be explained by the wet removal impact of the heavy
305 rain. It is well known that rains wash out the coarse particles, resulting in a fine size distribution (Dey et al.,
306 2004). The \AA value during EP-4 fluctuated between 0.08 and 0.2. Since the rains are light and short, the
307 clear days in EP-4 are more impacted by the north air mass, which brings in a larger fraction of coarse dust
308 particles. Comparatively, the \AA value was lower in both the haze and fog periods including EP-1, EP-3 and
309 EP-5. Especially in the case of EP-5, the low \AA value indicated that the biomass burning emission could
310 contain more coarse particles. Such scene is in contrast to the conclusion that the haze days were dominated
311 by fine particles (Yan et al., 2008). It is likely caused by the high collision occurrences of fine particles
312 along the long-range transport from the fire spots (Wang et al., 2009b). In comparison, the \AA value during
313 2001 to 2005 in Beijing altered between 0.04 and 1.06 (Yu et al., 2006). The lower limit is similar with the
314 present field-measurement, while the upper limit is much higher than this study. This could be attributed to
315 the increase of fine particle emission contributed by more vehicles, waste incineration and industrial plants
316 in the past years.

317 Single scattering albedo (SSA), ω , was defined as the ratio of the aerosol scattering coefficient (σ_{sca}) to
318 the extinction coefficient (σ_{ext}). This parameter is especially important in the estimation of direct aerosol
319 radiative forcing, since even a small error in its estimation might change the sign of aerosol radiative forcing
320 (Takemura et al., 2002). Figs. 3c and d show the time series of σ_{sca} , σ_{abs} , σ_{ext} and SSA at 550 nm during the

321 measurement period. The mean ω was 0.73, 0.82 and 0.79 in EP-2, EP-4, and EP-5, respectively, implying
322 that mineral dust in EP-4 accelerates the optical scattering while soot favours the optical absorption.
323 Compared with other reported results (Che et al., 2014; Li et al., 2007; Qian et al., 2007), the mean ω is
324 lower in this study, suggesting that more soot is uploaded into the atmosphere during this period. It is well
325 known that soot emission is much higher in the past years, mainly contributed by the residential coal
326 combustion, biomass burning, coke production, and diesel vehicles (Wang et al., 2012b). Especially, when
327 air masses moved from south direction the sampling site were influenced by heavy polluted air mass mixed
328 by soot, sulfate, and OC-components, from the dense population centres and industrial areas (Sun et al.,
329 2006; Wang et al., 2006), which was also confirmed by the TEM observation.

330 **3.3 Morphology and chemical composition of aerosols**

331 Based on morphology and chemical composition, 1173 particles were classified into nine categories: S-rich
332 (Fig. 4a), N-rich (Fig. 4b), mineral (Fig. 4c), K-rich (Fig. 4d), soot (Fig. 4e), tar ball (Fig.4f), organic
333 (Fig.4g), metal (Fig. 4h) and fly ash (Fig. 4i). The classification is similar to the work reported by Li and
334 Shao (2009).

335 The most common particles are sulphates and nitrates (Figs. 4a and b), which are of the size around 1.0
336 μm , and have a light scattering ability (Jacobson, 2001). Sulphates appeared as subrounded masses under
337 the TEM, which decomposed or evaporated under the electron beam exposure. Conventionally, they were
338 formed by the reaction of precursor SO_2 or H_2SO_4 with other gases or particles (Khoder, 2002). Nitrates
339 were mostly of scalloped morphology in the TEM images. They were relatively stable when exposed to the
340 electron beam. Nitrates formed through the homogeneous reaction with the precursor either NO_2 or
341 heterogenic reaction with HNO_3 (Khoder, 2002). (Pathak et al., 2004; Seinfeld and Pandis, 2012).

342 In the clear days, as the result of effects of northern air mass, dust particles were relatively abundant. The
343 size of dust particles (Fig. 4c) were large, usually bigger than 1.0 μm , so far as to 8.0 μm . Their compositions
344 differed from each other, mostly are silicates and calcium sulphate or carbonate, all of which were stable
345 under the exposure of the electron beam. Dust particles were reported to have a light scattering effect,

346 resulting in a negative aerosol radiative forcing (Wang et al., 2009b). They took up a large portion in EP-4,
347 impacted by the north wind taking along particles from the dusty regions.

348 As for the haze episode, K-rich particles (Li et al., 2010; Duan et al., 2004; Engling et al., 2009), soot (Li
349 et al., 2010), tar ball (Chakrabarty et al., 2010; Bond, 2001) and organic (Lack et al., 2012) were more
350 observed under the TEM. K-rich particles (Fig. 4d) often existed as sulphate or nitrate. A larger fraction of
351 K-rich particles was observed in EP-5 than those in the other periods. Together with the back trajectories
352 and fire spot maps, it was supposed that the regional haze occurred in EP-5 was contributed significantly
353 by the biomass burning. K-rich particles were characterized by the irregular shape, which was unstable
354 when exposed to electron beam. KCl was barely detected in the samples, even though it has been
355 recommended that KCl was internally mixed with K_2SO_4 and KNO_3 in fresh biomass burning plumes (Li
356 et al., 2010; Li et al., 2003; Adachi and Buseck, 2008). Based on the EDS data, K-rich particles in the present
357 work mostly consisted of N, Na, O, S, and K, whereas it was free of Cl, implying KCl could have suffered
358 from chemical reactions and transformed into sulphates or nitrates (Li and Shao, 2010). Such particles
359 displayed a negative climate forcing (Hauglustaine et al., 2014).

360 It was well documented that soot (Fig. 4e) was vital to light absorption, which could alter regional
361 atmospheric stability and vertical motions, the large scale circulation and precipitation with significant
362 regional climate effects (Ramanathan et al., 2001; Jacobson, 2002). It was well characterized by a structure
363 like onion ring, resembling a fractal long chain as agglomerates of small spherical monomers (Li and Shao,
364 2009). The fresh soot was loose and externally mixed. However, after undergoing a long-range
365 transportation and aging in the atmosphere, soot became more compacted, with a slight increase of O
366 concentration because of the photochemistry (Stanmore et al., 2001; Krasowsky et al., 2016). Meanwhile,
367 soot generally attached to other particles on the surface or serves as the core for other particle formation.

368 Tar ball (Fig. 4f) was present as a spherical carbon ball with a small fraction of O. It was thought to
369 origin from the smouldering combustion and have relatively strong absorption effects (Chakrabarty et al.,
370 2010; Bond, 2001). Tar balls constituted a large fraction of the fresh emitted wildfire carbonaceous particles
371 (China et al., 2013; Lack et al., 2012). But it was seldom observed in the present work, even in EP-5 when

372 there was severe biomass burning emission, which may be due to the difference in burning species and
373 conditions.

374 Organic matter (Fig. 4g) identified by HRTEM was amorphous species, and was stable under the strong
375 electron beam exposure. It could be traced to the direct emission such as biomass burning (Lack et al.,
376 2012), or the second reaction between VOCs with ozone (Wang et al., 2012a). It can absorb radiation in the
377 low-visible and UV wavelengths (Chakrabarty et al., 2010;Clarke et al., 2007;Lewis et al., 2008;Hoffer et
378 al., 2006). In addition, when compassing soot as the core, organic matter can enhance absorption by internal
379 mixing (Adachi and Buseck, 2008).

380 For the common haze and fog episodes, the stagnated weather favours the accumulation of pollutants,
381 especially metal particles and fly ash (Hu et al., 2015). Metal particles (Fig. 4h) were generally round and
382 stable under the TEM. Fly ash (Fig. 4i) was a dark sphere with large size of $> 1 \mu\text{m}$. It was a common
383 product of industrial activities in the northern China (Shi et al., 2003). As the complex refractive index
384 (CRI) indicated, metal oxide particles and fly ash can scatter light, but the former has a weak absorption
385 ability while the later has almost no light absorption ability (Ebert et al., 2004).

386 Figure 5 shows percentage of nine components in clear, haze and fog episodes under external mixing,
387 internal mixing and adjacent states (partially internal mixing). About 28% of particles were internally mixed
388 in the foggy days, while about 52% of particles exhibited external mixing state in clear days based on the
389 TEM analysis. Mineral particles were inclined to be externally mixed with K-rich particles and organic
390 matter in clear days, while the external ratio of other particles were relatively lower, particularly in the haze
391 and fog days. Li et al. (2010) showed that mineral particles generally displayed external association with
392 organic matter or other particles. However, many fine particles including metal-bearing particles, fly ash
393 and soot were often internally mixed with S-rich and K-rich particles, particularly during the fog-haze
394 episodes. Shi et al. (2008) reported that rapid aging of fresh soot tended to appear during the fog-haze days,
395 which were generally associated with ammonium sulfate. Heavy polluted air generally promoted the
396 coagulation between S/K-rich particles and those fine particles such as metal particles, soot, and fly ash (Li

397 and Shao, 2009), which could explain the results. Additionally, haze and fog episodes held a higher
398 possibility of collision and attachment due to the heavy particle loading and prolonged remaining in the
399 atmosphere (Li and Shao, 2009; Li et al., 2010), leading to a higher internal mixed state percentage around
400 65%.

401 **3.4 Optical properties related to morphological types of aerosols~~The relation of optical properties~~**
402 **~~and the morphologies of aerosol particles~~**

403 The different morphologies of the particles collected from the different weather can be easily identified
404 under the TEM, as shown in Fig. 6. Due to the washout effect of the heavy rain, the particles collected in
405 the typical clear period of EP-2 were much smaller in size (Figs. 6a, b), which was in good agreement with
406 the larger Ångström exponent. The coarse particles, such as dusts, were hardly observed, whereas a few K-
407 rich particles were detected, of which presented in small cubic shape. Such particles could be explained by
408 the coal combustion around the sampling site due to the slight fire spots presence. Besides, the cubic shape
409 of K-rich particles suggested they have not undergone long transportation or severe photochemical reaction
410 because cubic K-rich particles were generally generated from the molten nature of the material at high
411 temperatures (Ault et al., 2012). Likewise, soot was generally less oxidized in the EP-2 periods, maintaining
412 fractional morphologies and externally mixed. Small metal particles and amorphous Zn-particles dominated
413 the fine particles, which was ascribed to the industrial activity and/or waste incineration (Choël et al.,
414 2006;Moffet et al., 2008).

415 In the EP-5 episode, the increased aerosol loading played a remarkable role in the enhancement of
416 scattering coefficient and decrease of visibility (Kang et al., 2013; Charlson et al., 1987; Deng et al., 2008).
417 Because of the high rate of aerosol collision, particles were larger than those in the clear days (Figs. 6c, d),
418 leading to a smaller Ångström exponent. Almost of the soot particles observed under the TEM were
419 compact and adhesive. It was internally mixed with the K-rich particles, which were larger, rounder or with
420 a coating of high S components. As discussed above, they were probably transported from the south crop
421 residual burning and undergo the ageing in the atmosphere, confirmed by the trajectories passing through

422 intense fire spots. Due to the high concentration of soot, EP-5 were characterized by a high absorption
423 coefficient, shown in Fig. 3.

424 The BC variations in the different weather types during the sampling period were illustrated in Fig. 7.
425 The preliminary component of BC could be viewed as the soot. High BC concentration was easily
426 recognized in EP-5 with a mean value of $12.8 \mu\text{g m}^{-3}$, while it is low up to $1.04 \mu\text{g m}^{-3}$ during the clear
427 periods. The former is about 11.3 times higher than that of the latter, which is due to the lower boundary
428 layer. In comparison, absorption coefficient of EP-5 (468.7 Mm^{-1}) was about 94.7 times higher than that of
429 EP-4 (1.3 Mm^{-1}), more than 8 times of the BC ratio. It was supposed that BC was internally mixed with
430 other aerosols in the EP-5, which lead to the considerable elevation of absorption coefficient (Tan et al.,
431 2016). However, models estimated an enhancement of BC forcing up to a factor of 2.9 when BC is internally
432 mixed with other aerosols, compared with externally mixed scenarios (Jacobson, 2001), which was much
433 lower than this case. Accordingly, other light absorbing substances may contribute to the discrepancy. For
434 example, brown carbon is an indispensable component of biomass burning, which has a strong absorption
435 ability as well (Hoffer et al., 2006; Andreae and Gelencsér, 2006). Other particles such as dust may also
436 contribute to the over-enhanced absorption coefficient (Yang et al., 2009). Our observations were
437 agreement with the previous studies reported by (Wang et al., 2009b; Xia et al., 2006), which shows that
438 aerosol particles under hazy weather conditions generate a positive heating effect on the atmospheric. In the
439 foggy days of EP-3 episode, the high PM_{10} concentration and AOD caused significant increase of scattering
440 coefficient (Tan et al., 2016). Furthermore, metal-bearing particles and soot were internally associated with
441 some coatings including S-rich, N-rich and K-rich particles. Zhang et al. (2008) reported that coating with
442 sulphuric acid enhance the optical properties of soot aerosols. Furthermore, the collected particles displayed
443 larger size than those collected from the clear days under the TEM (Figs. 6e, f). The larger size particles in
444 the foggy days could be caused by hygroscopic growth under the high relative humidity, and the collision
445 among the overloading particles, which was likewise illustrated by the Ångström exponent shown in Fig.3.
446 Consequently, the larger particles enhance the scattering of sunlight, and lead to more apparent impairment
447 of visibility (Quan et al., 2011). Chow et al. (2002a) reported that RH also has a profound impact on

448 visibility. Some fan-like nitrate particles have inclusions which may act as the growth cores or be
449 encompassed during the hygroscopic growth. Bian et al. (2009) reported that whenever the RH is elevated,
450 its importance to AOD is substantially amplified if the particles are hygroscopic (Bian et al., 2009). Li et
451 al. (2010) found that soot particles became hydrophilic when they were coated with the water-soluble
452 compounds such as sulphates or nitrates, implying that soot can provide important nuclei for the
453 development of aerosol particles. Furthermore, Fig. 6e and f illustrate a large fraction of internally mixed
454 soot. It was not visible until being exposed to electron beam for a short time. As for an internally mixed
455 particle, sulphate and nitrate coatings act as a “focusing mirror”, and enhanced light absorption greatly.
456 Therefore, the BC concentration in foggy conditions was $6.12 \mu\text{g m}^{-3}$, and the absorption coefficient is 143.7
457 Mm^{-1} , which were 2.09 and 0.83 times of the hazy days, respectively. Model calculation also have
458 recommended that light absorption ability of the internally mixed soot particles were enhanced by 30%
459 than that of soot alone (Fuller et al., 1999). A variety of metal particles were also observed in the foggy
460 days, as foggy days had a stable low upper layer boundary and slight wind, leading to the accumulation of
461 pollutions. These pollution sources range from steel plants and waste incineration to vehicle emission and
462 so on (Hu et al., 2015).

463 **4 Conclusions**

464 The relationship between characteristics of aerosol particles and optical properties is of importance to
465 the atmospheric chemistry research. However, the relationship between characteristics of aerosol particles
466 and optical absorption remains poorly understood. Characteristics of aerosol optical properties,
467 morphologies and their relationship were studied in urban Beijing during the clear, haze and fog episodes,
468 sampled from 24th May to 22nd Jun, 2012. Transmission Electron Microscope (TEM), a Cavity Ring Down
469 Spectrometer (CRDS), a nephelometer and an aethalometer were employed to investigate the corresponding
470 changes of the aerosol properties. Five episodes were categorised according to the meteorological
471 conditions and composition. The results indicated that the clear episode (EP-2 and EP-4) was characterized
472 as the low aerosol Optical Depth ($\text{AOD} = 0.72$) and less pollutants compared with haze (1.14) and fog (2.92)
473 episodes, which are mostly externally mixed. The high Ångström exponent (> 2.0) suggests that coarse

474 particles were scarcely observed in EP-2 due to the washout of a previous heavy rain, whereas they were
475 widespread in EP-4 (Ångström exponent = 0.04), which had some mineral particles introduced from the
476 north. In contrast, industry-induced haze (EP-1) and biomass burning-induced haze (EP-5) were both
477 affected by the south air mass. Higher AOD values illustrated heavy loading particle concentrations. All of
478 the particles were classified into nine categories including S-rich, N-rich, mineral, K-rich, soot, tar ball,
479 organic, metal and fly ash based on the TEM analysis. In the haze episode, as the influence of severe crop
480 residue combustion, a large fraction of soot was detected, which sticks to sulphate or nitrate particles
481 transformed from KCl. Both black carbon (BC) acceleration, internally mixed effects, and other light
482 absorbing substances, contributed the light absorption enhancement. For foggy days, soot was mostly
483 internally mixed with sulphates and nitrates, which revealed themselves after electron exposure under the
484 TEM. The larger size distribution was likely to be caused by both hygroscopic growth and collision between
485 particles during the aging. About 28% of particles were internally mixed in the foggy days, which favored
486 the light absorption. The comparison of all the episodes provides a deeper insight of how mixing states
487 influence the aerosol extinction properties and also a clue to the air pollution control in the crop burning
488 seasons. The result presented herein is beneficial to air pollution control and prevention in China.

489 **ACKNOWLEDGMENTS**

490 This work was supported by National Natural Science Foundation of China (Nos. 21577022, 21190053,
491 40975074), Ministry of Science and Technology of China (2016YFC0202700), and International
492 cooperation project of Shanghai municipal government (15520711200).

493 **References**

494 Adachi, K., and Buseck, P.: Internally mixed soot, sulfates, and organic matter in aerosol particles from
495 Mexico City, *Atmos. Chem. Phys.*, 8, 6469-6481, 2008.
496 Adler, G., Riziq, A. A., Erlick, C., and Rudich, Y.: Effect of intrinsic organic carbon on the optical
497 properties of fresh diesel soot, *P. Natl. Acad. Sci. USA.*, 107, 6699-6704, 2010.

498 Alexander, D. T., Crozier, P. A., and Anderson, J. R.: Brown carbon spheres in East Asian outflow and
499 their optical properties, *Science*, 321, 833-836, 2008.

500 Anderson, T. L., and Ogren, J. A.: Determining aerosol radiative properties using the TSI 3563 integrating
501 nephelometer, *Aerosol Air Qual. Res.*, 29, 57-69, 1998.

502 Andreae, M., and Gelencsér, A.: Black carbon or brown carbon? The nature of light-absorbing
503 carbonaceous aerosols, *Atmos. Chem. Phys.*, 6, 3131-3148, 2006.

504 Ault A.P., Peters T.M., Sawvel E.J., Casuccio G.S., Willis R.D., Norris G.A., et al.: Single-particle SEM-
505 EDX analysis of iron-containing coarse particulate matter in an urban environment: sources and distribution
506 of iron within Cleveland, Ohio. *Environ Sci Technol.*, 46: 4331–4339, 2012.

507 Bahadur, R., Praveen, P. S., Xu, Y., and Ramanathan, V.: Solar absorption by elemental and brown carbon
508 determined from spectral observations, *P. Natl. Acad. Sci. USA.*, 109, 17366-17371, 2012.

509 Bian, H., Chin, M., Rodriguez, J., Yu, H., Penner, J. E., and Strahan, S.: Sensitivity of aerosol optical
510 thickness and aerosol direct radiative effect to relative humidity, *Atmos. Chem. Phys.*, 9, 2375-2386, 2009.

511 Bond, T. C.: Spectral dependence of visible light absorption by carbonaceous particles emitted from coal
512 combustion, *Geophys. Res. Lett.*, 28, 4075-4078, 2001.

513 Brown, A.J.: Spectral bluing induced by small particles under the Mie and Rayleigh regimes, *Lcarus.*, 239,
514 85-95, 2014.

515 Buseck, P. R., and Pofai, M.: Airborne minerals and related aerosol particles: Effects on climate and the
516 environment, *P. Natl. Acad. Sci. USA.*, 96, 3372-3379, 1999.

517 Carabali, G., Mamani-Paco, R., Castro, T., Peralta, O., Herrera, E., and Trujillo, B.: Optical properties,
518 morphology and elemental composition of atmospheric particles at T1 supersite on MILAGRO campaign,
519 *Atmos. Chem. Phys.*, 12, 2747-2755, 2012.

520 Chakrabarty, R., Moosmüller, H., Chen, L.-W., Lewis, K., Arnott, W., Mazzoleni, C., Dubey, M., Wold,
521 C., Hao, W., and Kreidenweis, S.: Brown carbon in tar balls from smoldering biomass combustion, *Atmos.*
522 *Chem. Phys.*, 10, 6363-6370, 2010.

523 Chameides, W. L., Yu, H., Liu, S., Bergin, M., Zhou, X., Mearns, L., Wang, G., Kiang, C., Saylor, R., and
524 Luo, C.: Case study of the effects of atmospheric aerosols and regional haze on agriculture: An opportunity
525 to enhance crop yields in China through emission controls?, *P. Natl. Acad. Sci. USA.*, 96, 13626-13633,
526 1999.

527 Charlson, R. J., Lovelock, J. E., Andreae, M. O., and Warren, S. G.: Oceanic phytoplankton, atmospheric
528 sulphur, cloud albedo and climate, *Nature*, 326, 655-661, 1987.

529 Che, H., Xia, X., Zhu, J., Li, Z., Dubovik, O., Holben, B., Goloub, P., Chen, H., Estelles, V., and Cuevas-
530 Agulló, E.: Column aerosol optical properties and aerosol radiative forcing during a serious haze-fog month
531 over North China Plain in 2013 based on ground-based sunphotometer measurements, *Atmos. Chem. Phys.*,
532 14, 2125-2138, 2014.

533 China, S., Mazzoleni, C., Gorkowski, K., Aiken, A. C., and Dubey, M. K.: Morphology and mixing state
534 of individual freshly emitted wildfire carbonaceous particles, *Nature commun.*, 4, 2013.

535 Choël, M., Deboudt, K., Flament, P., Lecornet, G., Perdrix, E., and Sobanska, S.: Fast evolution of
536 tropospheric Pb-and Zn-rich particles in the vicinity of a lead smelter, *Atmos. Environ.*, 40, 4439-4449,
537 2006.

538 Chow, J. C., Bachmann, J. D., Wierman, S. S., Mathai, C., Malm, W. C., White, W. H., Mueller, P. K.,
539 Kumar, N., and Watson, J. G.: Visibility: science and regulation, *J. Air. Waste Manage.*, 52, 973-999, 2002.

540 Clarke, A., McNaughton, C., Kapustin, V., Shinozuka, Y., Howell, S., Dibb, J., Zhou, J., Anderson, B.,
541 Brekhovskikh, V., and Turner, H.: Biomass burning and pollution aerosol over North America: Organic
542 components and their influence on spectral optical properties and humidification response, *J. Geophys.*
543 *Res.-Atmos.*, 112, 2007.

544 Deng, X., Tie, X., Wu, D., Zhou, X., Bi, X., Tan, H., Li, F., and Jiang, C.: Long-term trend of visibility and
545 its characterizations in the Pearl River Delta (PRD) region, China, *Atmos. Environ.*, 42, 1424-1435, 2008.

546 Dey, S., Tripathi, S. N., Singh, R. P., and Holben, B. N.: Influence of dust storms on the aerosol optical
547 properties over the Indo-Gangetic basin, *J. Geophys. Res.-Atmos.*, 109, 10.1029/2004jd004924, 2004.

548 Doran, J., Barnard, J. C., Arnott, W., Cary, R., Coulter, R., Fast, J. D., Kassianov, E. I., Kleinman, L.,
549 Laulainen, N. S., and Martin, T.: The T1-T2 study: evolution of aerosol properties downwind of Mexico
550 City, *Atmos. Chem. Phys.*, 7, 1585-1598, 2007.

551 Duan, F., Liu, X., Yu, T., and Cachier, H.: Identification and estimate of biomass burning contribution to
552 the urban aerosol organic carbon concentrations in Beijing, *Atmos. Environ.*, 38, 1275-1282, 2004.

553 Ebert, M., Weinbruch, S., Hoffmann, P., and Ortner, H. M.: The chemical composition and complex
554 refractive index of rural and urban influenced aerosols determined by individual particle analysis, *Atmos.*
555 *Environ.*, 38, 6531-6545, 2004.

556 Eck, T. F., Holben, B. N., Reid, J. S., Dubovik, O., Smirnov, A., O'Neill, N. T., Slutsker, I., and Kinne, S.:
557 Wavelength dependence of the optical depth of biomass burning, urban, and desert dust aerosols, *J.*
558 *Geophys. Res.-Atmos.*, 104, 31333-31349, 10.1029/1999jd900923, 1999.

559 Engling, G., Lee, J. J., Tsai, Y.-W., Lung, S.-C. C., Chou, C. C.-K., and Chan, C.-Y.: Size-resolved
560 anhydrosugar composition in smoke aerosol from controlled field burning of rice straw, *Aerosol Air Qual.*
561 *Res.*, 43, 662-672, 2009.

562 Fu, H., Zhang, M., Li, W., Chen, J., Wang, L., Quan, X., and Wang, W.: Morphology, composition and
563 mixing state of individual carbonaceous aerosol in urban Shanghai, *Atmos. Chem. Phys.*, 12, 693-707, 2012.

564 Fuller, K. A., Malm, W. C., and Kreidenweis, S. M.: Effects of mixing on extinction by carbonaceous
565 particles, *J. Geophys. Res.-Atmos.*, 104, 15941-15954, 1999.

566 Guo, L., Hu, Y., Hu, Q., Lin, J., Li, C., Chen, J., Li, L., and Fu, H.: Characteristics and chemical
567 compositions of particulate matter collected at the selected metro stations of Shanghai, China, *Sci. Total*
568 *Environ.*, 496, 443-452, 2014a.

569 Guo, Y., Feng, N., Christopher, S. A., Kang, P., Zhan, F. B., and Hong, S.: Satellite remote sensing of fine
570 particulate matter (PM_{2.5}) air quality over Beijing using MODIS, *Int. J. Remote Sens.*, 35, 6522-6544, 2014b.

571 Gustafsson, Ö., Kruså, M., Zencak, Z., Sheesley, R. J., Granat, L., Engström, E., Praveen, P., Rao, P., Leck,
572 C., and Rodhe, H.: Brown clouds over South Asia: biomass or fossil fuel combustion?, *Science*, 323, 495-
573 498, 2009.

574 Habib, G., Venkataraman, C., Bond, T. C., and Schauer, J. J.: Chemical, microphysical and optical
575 properties of primary particles from the combustion of biomass fuels, *Environ. Sci. Technol.*, 42, 8829-
576 8834, 2008.

577 Hand, J. L., Malm, W., Laskin, A., Day, D., Lee, T.-b., Wang, C., Carrico, C., Carrillo, J., Cowin, J. P., and
578 Collett, J.: Optical, physical, and chemical properties of tar balls observed during the Yosemite Aerosol
579 Characterization Study, *J. Geophys. Res.-Atmos.*, 110, 2005.

580 Hansen, A.: *The Aethalometer Manual*, Magee Sci., Berkeley, Calif, 2003.

581 Hoffer, A., Gelencsér, A., Guyon, P., Kiss, G., Schmid, O., Frank, G., Artaxo, P., and Andreae, M.: Optical
582 properties of humic-like substances (HULIS) in biomass-burning aerosols, *Atmos. Chem. Phys.*, 6, 3563-
583 3570, 2006.

584 Hu, Y., Lin, J., Zhang, S., Kong, L., Fu, H., and Chen, J.: Identification of the typical metal particles among
585 haze, fog, and clear episodes in the Beijing atmosphere, *Sci. Total Environ.*, 511, 369-380, 2015.

586 Hauglustaine, D.A., Balkanski, Y., Schulz, M.: A global model simulation of present and future nitrate
587 aerosols and their direct radiative forcing of climate, *Atmos. Chem. Phys.*, 14, 6863-6949, 2014.

588 Jacobson, M. Z.: Strong radiative heating due to the mixing state of black carbon in atmospheric aerosols,
589 *Nature*, 409, 695-697, 2001.

590 Jacobson, M. Z.: Control of fossil - fuel particulate black carbon and organic matter, possibly the most
591 effective method of slowing global warming, *J. Geophys. Res.-Atmos.*, 107, ACH 16-11-ACH 16-22, 2002.

592 Jeong, C.-H., Hopke, P. K., Kim, E., and Lee, D.-W.: The comparison between thermal-optical
593 transmittance elemental carbon and Aethalometer black carbon measured at multiple monitoring sites,
594 *Atmos. Environ.*, 38, 5193-5204, 2004.

595 Kang, H., Zhu, B., Su, J., Wang, H., Zhang, Q., and Wang, F.: Analysis of a long-lasting haze episode in
596 Nanjing, China, *Atmos. Res.*, 120, 78-87, 2013.

597 Krasowsky, T.S., McMeeking, G.R., Wang, D.B., Sioutas.C., Ban-Weiss, G.A.: Measurements of the
598 impact of atmospheric aging on physical and optical properties of ambient black carbon particles in Los
599 Angeles, *Atmos. Environ.*, 142, 496-504, 2016.

600 Katrinak, K. A., Rez, P., Perkes, P. R., and Buseck, P. R.: Fractal geometry of carbonaceous aggregates
601 from an urban aerosol, *Environ. Sci. Technol.*, 27, 539-547, 1993.

602 Khoder, M.: Atmospheric conversion of sulfur dioxide to particulate sulfate and nitrogen dioxide to
603 particulate nitrate and gaseous nitric acid in an urban area, *Chemosphere*, 49, 675-684, 2002.

604 Kleinman, L. I., Daum, P. H., Lee, Y. N., Senum, G. I., Springston, S. R., Wang, J., Berkowitz, C., Hubbe,
605 J., Zaveri, R. A., and Brechtel, F. J.: Aircraft observations of aerosol composition and ageing in New
606 England and Mid - Atlantic States during the summer 2002 New England Air Quality Study field campaign,
607 *J. Geophys. Res.-Atmos.*, 112, 2007.

608 Lack, D. A., Langridge, J. M., Bahreini, R., Cappa, C. D., Middlebrook, A. M., and Schwarz, J. P.: Brown
609 carbon and internal mixing in biomass burning particles, *P. Natl. Acad. Sci. USA.*, 109, 14802-14807,
610 10.1073/pnas.1206575109, 2012.

611 Langridge, J. M., Lack, D., Brock, C. A., Bahreini, R., Middlebrook, A. M., Neuman, J. A., Nowak, J. B.,
612 Perring, A. E., Schwarz, J. P., and Spackman, J. R.: Evolution of aerosol properties impacting visibility and
613 direct climate forcing in an ammonia - rich urban environment, *J. Geophys. Res.-Atmos.*, 117, 2012.

614 Lei, T., Zuend, A., Wang, W., Zhang, Y., and Ge, M.: Hygroscopicity of organic compounds from biomass
615 burning and their influence on the water uptake of mixed organic–ammonium sulfate aerosols, *Atmos.*
616 *Chem. Phys.*, 14, 11625-11663, 2014.

617 Lewis, K., Arnott, W. P., Moosmüller, H., and Wold, C. E.: Strong spectral variation of biomass smoke
618 light absorption and single scattering albedo observed with a novel dual - wavelength photoacoustic
619 instrument, *J. Geophys. Res.-Atmos.*, 113, 2008.

620 Li, C., Marufu, L. T., Dickerson, R. R., Li, Z., Wen, T., Wang, Y., Wang, P., Chen, H., and Stehr, J. W.: In
621 situ measurements of trace gases and aerosol optical properties at a rural site in northern China during East

622 Asian Study of Tropospheric Aerosols: An International Regional Experiment 2005, *J. Geophys. Res.-*
623 *Atmos.*, 112, 2007.

624 Li, J., Pósfai, M., Hobbs, P. V., and Buseck, P. R.: Individual aerosol particles from biomass burning in
625 southern Africa: 2, Compositions and aging of inorganic particles, *J. Geophys. Res.-Atmos.*, 108, 2003.

626 Li, W., and Shao, L.: Transmission electron microscopy study of aerosol particles from the brown hazes in
627 northern China, *J. Geophys. Res.-Atmos.*, 114, 2009.

628 Li, W., and Shao, L.: Direct observation of aerosol particles in aged agricultural biomass burning plumes
629 impacting urban atmospheres, *Atmos. Chem. Phys.*, 10, 10589-10623, 2010.

630 Li, W., Shao, L., and Buseck, P.: Haze types in Beijing and the influence of agricultural biomass burning,
631 *Atmos. Chem. Phys.*, 10, 8119-8130, 2010.

632 Li, W., Shao, L.: Characterization of mineral particles in winter fog of Beijing analyzed by TEM and SEM.
633 *Environ. Monit. Assess.*, 161, 565-573, 2010.

634 Moffet, R. C., Desyaterik, Y., Hopkins, R. J., Tivanski, A. V., Gilles, M. K., Wang, Y., Shutthanandan, V.,
635 Molina, L. T., Abraham, R. G., and Johnson, K. S.: Characterization of aerosols containing Zn, Pb, and Cl
636 from an industrial region of Mexico City, *Environ. Sci. Technol.*, 42, 7091-7097, 2008.

637 Moffet, R. C., and Prather, K. A.: In-situ measurements of the mixing state and optical properties of soot
638 with implications for radiative forcing estimates, *P. Natl. Acad. Sci. USA.*, 106, 11872-11877, 2009.

639 Pathak, R. K., Yao, X., and Chan, C. K.: Sampling artifacts of acidity and ionic species in PM_{2.5}, *Environ.*
640 *Sci. Technol.*, 38, 254-259, 2004.

641 Peppler, R., Bahrmann, C., Barnard, J. C., Laulainen, N., Turner, D., Campbell, J., Hlavka, D., Cheng, M.,
642 Ferrare, R., and Halthore, R.: ARM Southern Great Plains site observations of the smoke pall associated
643 with the 1998 Central American fires, *B. Am. Meteorol. Soc.*, 81, 2563-2591, 2000.

644 Qian, Y., Wang, W., Leung, L. R., and Kaiser, D. P.: Variability of solar radiation under cloud - free skies
645 in China: The role of aerosols, *Geophys. Res. Lett.*, 34, 2007.

646 Quan, J., Zhang, Q., He, H., Liu, J., Huang, M., and Jin, H.: Analysis of the formation of fog and haze in
647 North China Plain (NCP), *Atmos. Chem. Phys.*, 11, 8205-8214, 2011.

648 Ram, K., Sarin, M., and Tripathi, S.: Temporal trends in atmospheric PM_{2.5}, PM₁₀, elemental carbon,
649 organic carbon, water-soluble organic carbon, and optical properties: impact of biomass burning emissions
650 in the Indo-Gangetic Plain, *Environ. Sci. Technol.*, 46, 686-695, 2012.

651 Ramana, M., Ramanathan, V., Feng, Y., Yoon, S., Kim, S., Carmichael, G., and Schauer, J.: Warming
652 influenced by the ratio of black carbon to sulphate and the black-carbon source, *Nat. Geosci.*, 3, 542-545,
653 2010.

654 Ramanathan, V., Crutzen, P. J., Lelieveld, J., Mitra, A., Althausen, D., Anderson, J., Andreae, M., Cantrell,
655 W., Cass, G., and Chung, C.: Indian Ocean Experiment: An integrated analysis of the climate forcing and
656 effects of the great Indo-Asian haze, 2001.

657 Ramanathan, V., Chung, C., Kim, D., Bettge, T., Buja, L., Kiehl, J., Washington, W., Fu, Q., Sikka, D.,
658 and Wild, M.: Atmospheric brown clouds: Impacts on South Asian climate and hydrological cycle, *P. Natl.*
659 *Acad. Sci. USA.*, 102, 5326-5333, 2005.

660 Ramanathan, V., Ramana, M. V., Roberts, G., Kim, D., Corrigan, C., Chung, C., and Winker, D.: Warming
661 trends in Asia amplified by brown cloud solar absorption, *Nature*, 448, 575-578, 2007.

662 Roden, C. A., Bond, T. C., Conway, S., and Pinel, A. B. O.: Emission factors and real-time optical
663 properties of particles emitted from traditional wood burning cookstoves, *Environ. Sci. Technol.*, 40, 6750-
664 6757, 2006.

665 Saleh, R., Adams, P.J., Donahue, N.M., Robinson, A.L.: The interplay between assumed morphology and
666 the direct radiative effect of light-absorbing organic aerosol, *Geophys. Res. Lett.* 43, 8735–8743, 2016.

667 Seinfeld, J. H., and Pandis, S. N.: *Atmospheric chemistry and physics: from air pollution to climate change*,
668 John Wiley & Sons, 2012.

669 Shi, Z., Shao, L., Jones, T. P., Whittaker, A., Lu, S., Berube, K. A., He, T., and Richards, R. J.:
670 Characterization of airborne individual particles collected in an urban area, a satellite city and a clean air
671 area in Beijing, 2001, *Atmos. Environ.*, 37, 4097-4108, 2003.

672 Shi, Z. B., D. Z. Zhang, H. Z. Ji, S. Hasegawa, and M. Hayashi.: Modification of soot by volatile species
673 in an urban atmosphere, *Sci. Total Environ.*, 389, 195–201, 2008.

674 Shingler, T., Sorooshian, A., Ortega, A., Crosbie, E., Wonaschütz, A., Perring, A.E.: Ambient observations
675 of hygroscopic growth factor and $f(\text{RH})$ below 1: Case studies from surface and airborne measurements, *J.*
676 *Geophys. Res.*, 121, 13661-13677, 2016.

677 Solomon, S.: *Climate change 2007-the physical science basis: Working group I contribution to the fourth*
678 *assessment report of the IPCC*, Cambridge University Press, 2007.

679 Stanmore, B., Brillhac, J., and Gilot, P.: The oxidation of soot: a review of experiments, mechanisms and
680 models, *Carbon*, 39, 2247-2268, 2001.

681 Sun, Y., Zhuang, G., Tang, A., Wang, Y., and An, Z.: Chemical characteristics of PM_{2.5} and PM₁₀ in haze-
682 fog episodes in Beijing, *Environ. Sci. Technol.*, 40, 3148-3155, 2006.

683 Takemura, T., Nakajima, T., Dubovik, O., Holben, B. N., and Kinne, S.: Single-scattering albedo and
684 radiative forcing of various aerosol species with a global three-dimensional model, *J. Climate.*, 15, 333-
685 352, 2002.

686 Tan, H.B., Liu, L., Fan, S.J., Li, F., Yin, Y., Cai, M.F., Chan, P.W., 2016. Aerosol optical properties and
687 mixing state of black carbon in the Pearl River Delta, China, *Atmos. Environ.*, 131, 196-208, 2016.

688 Wang, G., Kawamura, K., Xie, M., Hu, S., Cao, J., An, Z., Waston, J. G., and Chow, J. C.: Organic
689 molecular compositions and size distributions of Chinese summer and autumn aerosols from Nanjing:
690 Characteristic haze event caused by wheat straw burning, *Environ. Sci. Technol.*, 43, 6493-6499, 2009a.

691 Wang, H., He, C., Morawska, L., McGarry, P., and Johnson, G.: Ozone-initiated particle formation, particle
692 aging, and precursors in a laser printer, *Environ. Sci. Technol.*, 46, 704-712, 2012a.

693 Wang, R., Tao, S., Wang, W., Liu, J., Shen, H., Shen, G., Wang, B., Liu, X., Li, W., and Huang, Y.: Black
694 carbon emissions in China from 1949 to 2050, *Environ. Sci. Technol.*, 46, 7595-7603, 2012b.

695 Wang, X., and Chen, J.: Fog Formation in Cold Season in Ji’nan, China: Case Analyses with
696 Application of HYSPLIT Model, *Adv. Meteorol.*, 2014, 8, 10.1155/2014/940956, 2014.

697 Wang, X., Xu, B., and Ming, J.: An overview of the studies on black carbon and mineral dust deposition in
698 snow and ice cores in East Asia, *J. Meteorol. Res.*, 28, 354-370, 10.1007/s13351-014-4005-7, 2014.

699 Wang, Y., Zhuang, G., Sun, Y., and An, Z.: The variation of characteristics and formation mechanisms of
700 aerosols in dust, haze, and clear days in Beijing, *Atmos. Environ.*, 40, 6579-6591, 2006.

701 Wang, Y., Che, H., Ma, J., Wang, Q., Shi, G., Chen, H., Goloub, P., and Hao, X.: Aerosol radiative forcing
702 under clear, hazy, foggy, and dusty weather conditions over Beijing, China, *Geophys. Res. Lett.*, 36, 2009b.

703 Wu, D., Mao, J., Deng, X., Tie, X., Zhang, Y., Zeng, L., Li, F., Tan, H., Bi, X., and Huang, X.: Black
704 carbon aerosols and their radiative properties in the Pearl River Delta region, *Science in China Series D:
705 Earth Sciences*, 52, 1152-1163, 2009.

706 Xia, X., Chen, H., Wang, P., Zhang, W., Goloub, P., Chatenet, B., Eck, T., and Holben, B.: Variation of
707 column - integrated aerosol properties in a Chinese urban region, *J. Geophys. Res.-Atmos.*, 111, 2006.

708 Yan, P., Tang, J., Huang, J., Mao, J., Zhou, X., Liu, Q., Wang, Z., and Zhou, H.: The measurement of
709 aerosol optical properties at a rural site in Northern China, *Atmos. Chem. Phys.*, 8, 2229-2242, 2008.

710 Yang, M., Howell, S., Zhuang, J., and Huebert, B.: Attribution of aerosol light absorption to black carbon,
711 brown carbon, and dust in China—interpretations of atmospheric measurements during EAST-AIRE, *Atmos.
712 Chem. Phys.*, 9, 2035-2050, 2009.

713 Yu, X., Cheng, T., Chen, J., and Liu, Y.: A comparison of dust properties between China continent and
714 Korea, Japan in East Asia, *Atmos. Environ.*, 40, 5787-5797, 2006.

715 Zhang, R., Khalizov, A. F., Pagels, J., Zhang, D., Xue, H., and McMurry, P. H.: Variability in morphology,
716 hygroscopicity, and optical properties of soot aerosols during atmospheric processing, *P. Natl. Acad. Sci.
717 USA.*, 105, 10291-10296, 2008.

718 Zhang, W., Zhuang, G., Guo, J., Xu, D., Wang, W., Baumgardner, D., Wu, Z., and Yang, W.: Sources of
719 aerosol as determined from elemental composition and size distributions in Beijing, *Atmos. Res.*, 95, 197-
720 209, <http://dx.doi.org/10.1016/j.atmosres.2009.09.017>, 2010.

721

722

723

724 **Table 1** Details about the analysed samples on the sSampling time; and instantaneous meteorological state
 725 and the number of particle analysed in each sample.

Sampling Time (BST ^a)			Conditions	RH (%)	Temp. (°C)	Wind		Visibility (km)	No.
Date	Starting	Duration				Speed (m/s)	Direction		
25-05-2012	13:40	4 min	Clear	20	29	2	160	-	136
30-05-2012	9:31	16 min	Clear	29	24	7	350	-	92
02-06-2012	9:00	1 min	Mist ^b	83	20	4	180	2	146
02-06-2012	13:27	2 min	Clear	48	27	4	190	-	138
03-06-2012	10:13	15 s	Fog	88	22	1	variable	1.2	110
18-06-2012	18:52	2 min	Haze	55	29	3	140	3	172
19-06-2012	9:10	2 min	Haze	61	25	1	variable	2.8	120
21-06-2012	9:10	1 min	Haze	69	26	2	110	2.2	117
23-06-2012	12:45	2 min	Mist ^b	84	25	4	120	3	142

^aBeijing standard time (8 h prior to GMT).

^bMist is studied here as fog.

726

727

728 **Figure captions**

729 **Figure 1.** 5 episodes categorization. EP-1 features haze induced mainly from transportation of south
730 industrial pollution, EP-2 clear, EP-3 frequent transition among haze, fog and clear conditions, EP-4 clear
731 with rain interrupted, and EP-5 haze resulted mainly from the biomass burning (Brown, green, and orange
732 colour mean the haze, clear, and fog conditions, respectively).

733 **Figure 2.** The 3-day back-trajectory clusters of each episode, arriving at Beijing at the height of 100 m,
734 together with the fire spot distribution of these periods (Green, purple, red, and blue line denotes the air
735 parcel with the height of 500, 1000, 2000, and 3000 m).

736 **Figure 3.** TEM typical views of the particles in clear (upper panel), haze (middle panel) and fog episodes
737 (bottom panel). 9 components are marked with the colourful arrows. (a1) (b1) (c1) (d1) (e1) (f1) is obtained
738 before the electron exposure and (a2) (b2) (c2) (d2) (e2) (f2) is after exposure. A fraction of S-rich particles
739 and other unstable particles decompose after electron exposure. Variation of optical parameters during the
740 study period. (a) Total Aerosol optical depth (AOD), and AOD resulted from Mie scatter and Rayleigh
741 scatter; (b) Ångström exponent (\AA) computed from the pairs of 700 nm and 450 nm, 700 nm and 550 nm,
742 and 550 nm and 450 nm; (c) light extinction, absorption and scattering coefficients; (d) calculated single
743 scattering albedo (SSA).

744 **Figure 4.** 9 categories of particles under the TEM view. The inserted spectra are obtained by the EDS, and
745 the grid like images are acquired from the SAED. (a) S-rich, (b) N-rich, (c) mineral, (d) K-rich, (e) soot, (f) tar
746 ball, (g) organic, (h) metal, (i) fly ash.

747 **Figure 5.** Variation of optical parameters during the study period. (a) Total Aerosol optical depth (AOD),
748 and AOD resulted from Mie scatter and Rayleigh scatter; (b) Ångström exponent (\AA) computed from the
749 pairs of 700 nm and 450 nm, 700 nm and 550 nm, and 550 nm and 450 nm; (c) light extinction, absorption
750 and scattering coefficients; (d) calculated single scattering albedo (SSA). Percentages of 9 particle
751 components under clear, haze and fog conditions with different mixing states.

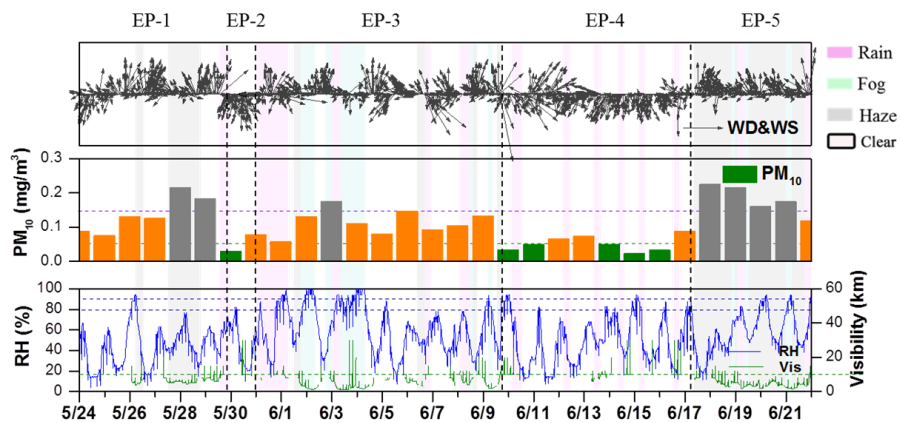
带格式的: 字体: 非加粗

752 **Figure 6.** TEM typical views of the particles in clear (upper panel), haze (middle panel) and fog episodes
753 (bottom panel). 9 components are marked with the colourful arrows. (a1) (b1) (c1) (d1) (e1) (f1) is obtained
754 before the electron exposure and (a2) (b2) (c2) (d2) (e2) (f2) is after exposure. A fraction of S-rich particles
755 and other unstable particles decompose after electron exposure. ~~Percentages of 9 particle components under~~

756 ~~clear, haze and fog conditions with different mixing states.~~

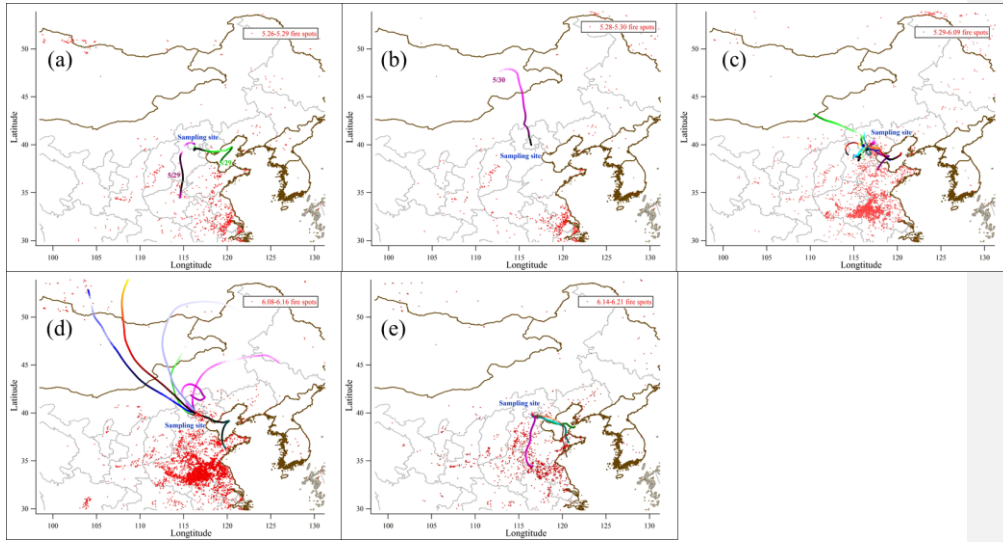
757 **Figure 7.** BC concentrations converted from the data measured by AE-31 and MAAP. Good correlation is
758 observed.

759



760
 761
 762
 763
 764
 765
 766
 767
 768
 769
 770
 771
 772

Figure 1



773

774

775

776

777

778

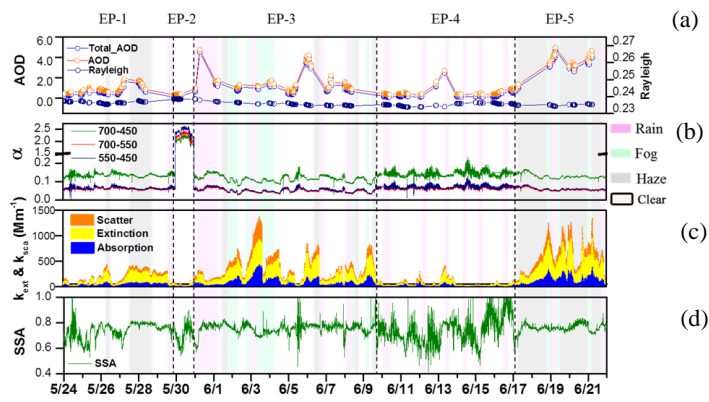
779

780

Figure 2

781

782



783

784

785

786

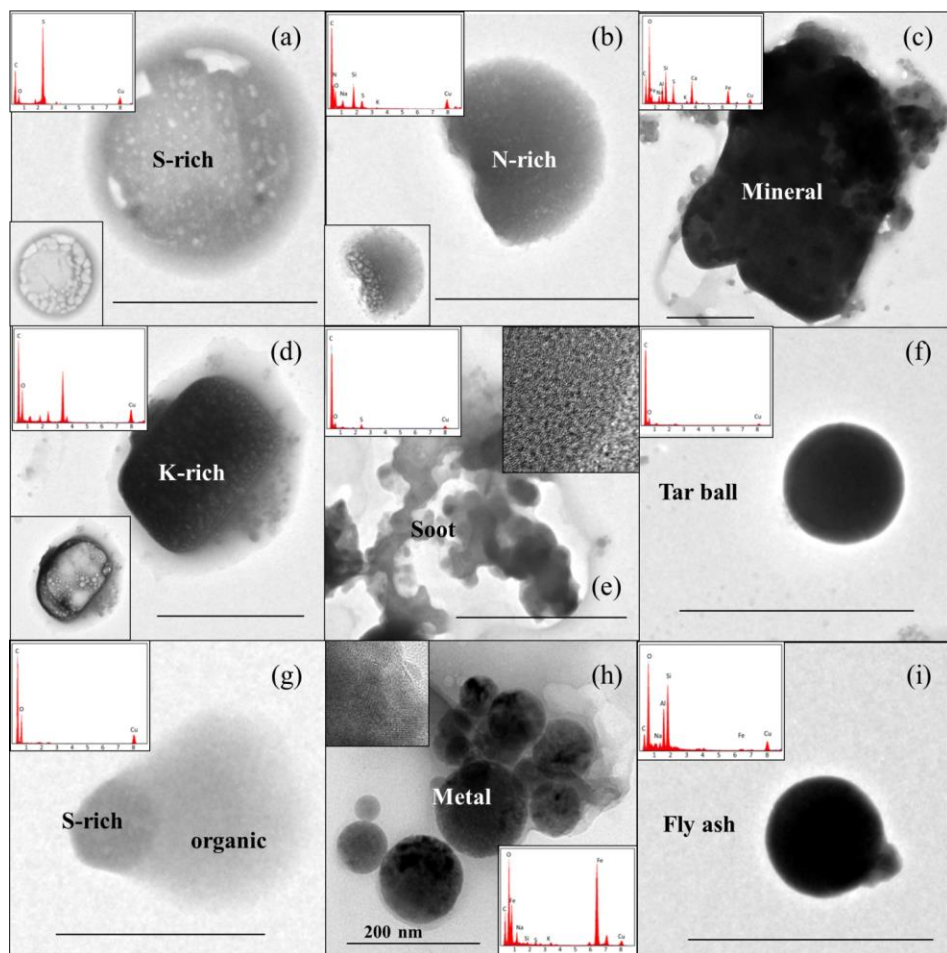
787

788

789

Figure 3

790



791

792

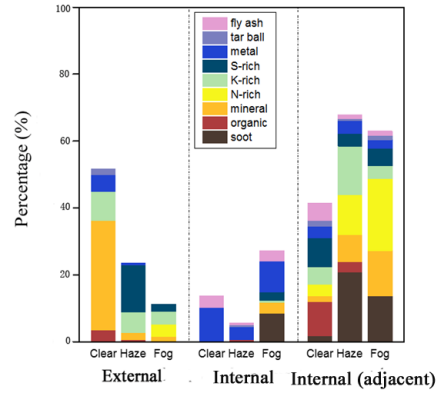
793

794

795

796

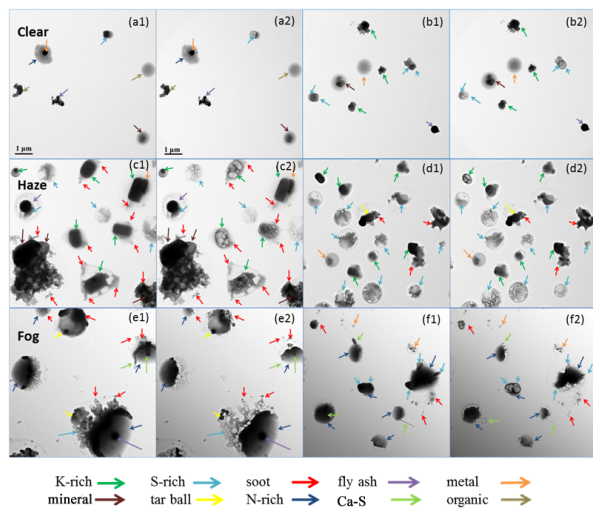
Figure 4



797
798
799
800

Figure 5

801



802

803

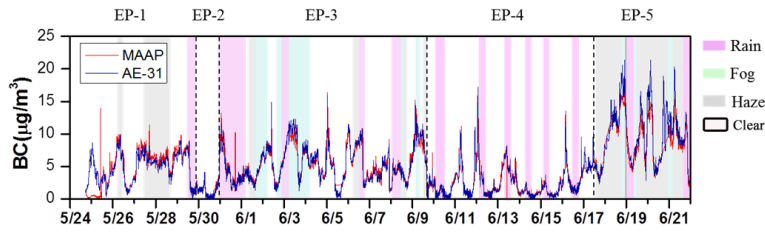
804

805

806

807

Figure 6



808
 809
 810
 811
 812
 813
 814
 815
 816
 817
 818

Figure 7